Bulletin of the New Zealand Society for Earthquake Engineering, Vol. 54, No. 4, December 2021

RECYCLING OF DAMAGED RC FRAMES: REPLACING CRUMBLED CONCRETE AND INSTALLING STEEL HAUNCHES BELOW/ABOVE THE BEAM AT CONNECTIONS

Naveed Ahmad[1], Arifullah[2], Babar Ilyas[2] and Sida Hussain[2]

(Submitted *April 2020*; Reviewed *June 2020*; Accepted *April 2021*)

ABSTRACT

Experimental and numerical studies are presented evaluating the efficacy of a recycling technique applied to a 1:3 reduced scale damaged RC frame. The crumbled concrete at the beam-column connections was replaced with new high-strength concrete. Epoxy mortar was applied at the interface to secure bonding between the old and new concrete. Additionally, the connections were provisioned with steel haunches, applied below and above the beams. The retrofitted frame was tested under quasi-static cyclic loads. The lateral resistance-displacement hysteretic response of the tested frame was obtained to quantify hysteretic damping, derive the lateral resistance-displacement capacity curve, and develop performance levels. The technique improved the response of the frame; exhibiting an increase in the lateral stiffness, resistance and post-yield stiffness of the frame in comparison to the undamaged original frame. This good behaviour is attributed to the steel haunches installed at connections. A representative numerical model was calibrated in the finite element program SeismoStruct. A set of spectrum compatible ground motions were input to the numerical model for response history analysis. The story drift demands were computed for both the design basis and maximum considered earthquakes. Moreover, the technique was extended to a five-story frame, which was evaluated through nonlinear static pushover and response history analyses. Overstrength factor $\Omega_R = 4.0$ is proposed to facilitate analysis and preliminary design of steel haunches and anchors for retrofitting the low-/mid-rise RC frames.

INTRODUCTION

The recent damaging earthquakes have raised concerns among designers regarding the critically damaged RC frames. As it is challenging to decide, whether to repair and retrofit (recycle) or demolish and rebuild (reconstruct)? The first option has the advantage to recycle damaged RC frames that would otherwise be demolished, having economic implications and has a significant impact on the environment by increasing the carbon foot print. However, such a decision is always difficult due to several issues including the limited budget and lack of resources that hamper the implementation of recycling techniques. Therefore, it is always desired to select an appropriate low-cost solution. Experimental studies have revealed that the application of epoxy for cracks repair have exhibited limited success in restoring the stiffness and resistance-displacement hysteretic response of damaged RC structures [1]. Many other conventional and advanced techniques, although effective in restoring lateral resistance of structures [1-4], were found practically invasive and labour-intensive.

Pampanin and Christopoulos [5] proposed a less invasive haunch retrofitting technique to protect the joints from incurring extensive damage. This technique composed of a diagonal metallic haunch element installed at the beam-column connection. This element stiffen the beam-column connection and reduce demands on joint panel. A simplified analytical procedure was presented for the retrofit design of strengthening exterior beam-column joint sub-assemblies. The assembly had plain round bars with limited transverse reinforcement in joint reinforcement and was detailed disproportionally. The technique was validated through quasi-static cyclic tests performed on 2:3 reduced scale beam-column joint sub-assemblies [6-7]; exhibiting an increase in strength and energy dissipation of retrofitted specimen in comparison to the as-built connection. This technique was further simplified using fully fastened haunches connected through direct post-installed anchors [8]. The later was called fully fastened haunch retrofit solutions (FFHRS). However, this also necessitated proper consideration of tension-stiffness and shear-stiffness of post-installed anchors into the design model. The effectiveness of the FFHRS is largely dependent on the efficiency of post-installed anchors, as confirmed through experimental tests on beam-column joint sub-assemblies and portal frames [9-10].

Khalili et al [11] confirmed the beneficial role of the stiffer haunch element through numerical analysis of the finite element-based frame model; lateral strength increases with the increase in the cross-sectional area of the haunch element. However, the technique reduced the deformation capacity of the frame, therefore, the increase in stiffness of the haunch element caused a reduction in translation ductility ratio and ductility factor. Kheyroddin et al. [12] proposed confining steel plates (revival sheets) to contain beam for increasing strength, post-yield stiffness, and energy dissipation capacity of the connection, as confirmed through experimental tests performed on beam-column joint sub-assemblies. Kanchanadevi and Ramanjaneyulu [13-14] experimentally investigated the effectiveness of a single haunch provided below the beam. It was found that the technique hampers the anchorage failure of bars at the joint, delays joint shear damage and increases the connection energy dissipation up to 2.30 times. Similarly, Zabihi et al. [15-16] also confirmed the efficacy of providing only a single haunch below the beam.

Akbar et al. [17] optimized the design of FFHRS; using channels provisioned with both direct and dowel anchors for attaching haunch to beam/column members. This was intended

[1] *Corresponding Author, Associate Professor, Department of Civil Engineering, UET Peshawar.* naveed.ahmad@uetpeshawar.edu.pk
[2] *MSc Scholar, Department of Civil Engineering, UET Peshawar.*

to reduce tension and shear demands on post-installed anchors. The validation was carried out through series of shake table tests performed on 1:3 reduced scale frame models. The tested frames exhibited an increase in the overstrength and response modification factor *R* of frames; an increase varying from 60% to 120% was observed. This is advantageous in reducing design level seismic forces in beam/column members. This was confirmed through shake-table tests performed on frames resisting input motions having peak horizontal acceleration up to 1.0g. Response history analyses were performed on the finite element based inelastic models using a set of ground motions to derive seismic fragility functions and loss curves. These demonstrated that the technique improves the seismic performance of as-built frames; resisting input motions with a higher intensity before exceeding the code permissible story-drift [18]. However, the later studies have demonstrated that the use of double haunches i.e. haunch provided both below and above the beam, are relatively effective in improving the seismic performance of the frame [17-18]. It is because of the tensile strain in the longitudinal bars of the column and the associated compression at the compressed toe of the section. This strain penetration within the joint core causes shear demand on the joint panel, therefore, incurs cracking and damage in the joint. Moreover, due to the low-strength of concrete, pry-out failure of concrete was observed. This was followed by the pull-out of anchors. Nevertheless, it happened at input base motions larger than ground motions corresponding to the design basis and maximum considered earthquakes. Wang et al. [19] and Akbar et al. [17] also investigated dissipating buckling restrained haunches that allowed the diagonal element to dissipate seismic energy for controlling seismic demands on the frame. However, the limited deformability of locally available steel material conforming to ASTM A36 may limit the hysteretic energy dissipation offered by haunches [20]. Therefore, a ductile haunch element should be used in case of dissipating haunches for a stable hysteretic response [19].

Retrofitting of RC frames using steel haunches have shown promising behaviour in improving seismic performance. However, its applicability in restoring, and possibly improving, seismic performance of critically damaged RC frames needs to be evaluated. The present research investigated the adequacy of a recycling technique for a critically damaged RC frame. Experimental in-plane quasi-static cyclic tests were performed on 1:3 reduced scale RC frame. Also, response history analysis was performed for representative inelastic numerical models to evaluate the performance of frame for various earthquake motions. The present research also proposed, and confirmed, a simple code-based procedure for seismic analysis and preliminary design of steel haunches for strengthening of critically damaged RC frames.

DESCRIPTION OF SELECTED RC FRAME AND STRENGTHENING PROCESS

Preliminary Design of Prototype RC Frame

Figure 1 reports the prototype of selected frame, which is representative of modern earthquake-resistant low-rise RC moment-resisting frames in Pakistan. The total seismic weight of the frame is equal to 633 kN that comprised of dead load and portion of the live load. The basic material properties considered for the design of the prototype frame are given in Table 1. The selected frame was analysed and designed using the equivalent lateral load analysis procedure given in the BCP-SP [21], and the design requirements given in the ACI-318-05 for the special moment-resisting frame (SMRF). However, the selected frame doesn't fulfil the requirement for development length of longitudinal beam bars. Also, the code suggests to take the column dimension parallel to the beam reinforcement not less than $20d_b$, where d_b is the diameter of the largest longitudinal beam bar. These were considered so that the test frame incorporate the construction deficiencies found in the field. Table 2 contains the basic dynamic properties of the prototype frame.

Table 1: Material properties assumed for the design of prototype reinforced concrete frame.

Property	Compressive Strength (MPa)	Young's Modulus (MPa)	Poisson's Ratio	Yield Strength (MPa)	Maximum Strength (MPa)
Concrete	21	21.52 GPa	0.20	-	-
Re-bars	-	200 GPa	0.30	414	621

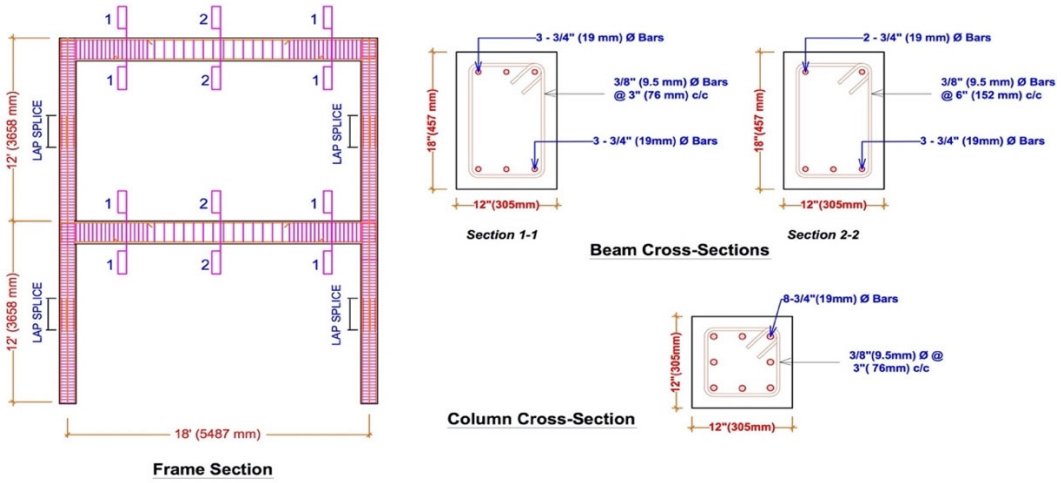

Figure 1: Geometric and reinforcement details of the prototype reinforced concrete moment-resisting frame.

Table 2: Dynamic properties determined for the prototype reinforced concrete frame.

Property	Seismic Weight (kN)	Effective Seismic Weight (kN)	Modal Participation Factor	Vibration Period (Sec)	
				Modal	Max. Allowed
Value	633	528	1.19	0.80	0.42

The design base shear force V_D was calculated using Equation (1), given in BCP-SP [21]:

$$V_D = \frac{C_V I}{RT} W \quad (1)$$

where C_V is the seismic coefficient, W is the seismic weight of the structure, I is the importance factor (which is 1.0 for standard occupancy structures), R is the response modification factor (R = 8.50 for SMRF). Table 3 contains the seismicity and structural data for standard occupancy structures in a high seismic zone. V_D = 70 kN was obtained for the considered prototype frame. A force equal to 2/3rd of base shear was applied at the roof and 1/3rd of base shear was applied at the first-floor level.

Under the design forces, the first-floor level beam develops a maximum bending moment demand equal to 94 kN-m. This beam is provided with 3#6 (19mm ϕ) top/bottom longitudinal bars. This gives a nominal moment capacity equal to 96 kN-m. The slab effect was not included at the design stage, which is a deficiency in the field [22]. The corresponding maximum moment developed at the base of the ground-story columns is equal to 70 kN-m. Therefore, the columns were provided with 8#6 (19mm ϕ) longitudinal steel bars. This gives nominal moment capacity of 73 kN-m, which is sufficient. The #3 (9.5mm ϕ) hoops of both the columns and beams were spaced at 76 mm on center with the first one located at 50 mm from the face of the support.

Moreover, the code (BCP-SP [21]) also recommends to satisfy the requirement given in Equation (2):

$$\left(\frac{6/5 M_b}{M_c} \leq 1 \right) \quad (2)$$

where M_b is the moment capacity of beams and M_c is the total moment capacity of columns (both below and above the beams). This was found equal to 0.70 at first-floor connection. As this is less than 1.0, therefore, it is expected to avoid flexural hinging at the top end of columns. The code allows plastic-hinges to form at the base of ground-story columns under design base earthquake. Therefore, a simple static equilibrium consideration will reveal the column top-end flexure capacity should be greater than 0.75 times the beam flexure capacity. This will avoid flexural hinging at the top end of ground-story columns. In the present case, the ratio of flexure capacity of the top end of ground-story columns to the beam flexure capacity is 0.86, which is approximately 15% higher than the required.

Preparation of 1:3 Reduced Scale Test Frame

The selected frame was scaled down by considering scale factor S_L equal to 3 for preparing 1:3 reduced scale frame for experimental testing. Simple model idealization was adopted, therefore, only the dimensions of structural components (beams and columns) and diameter of bars were reduced. The test frame was provisioned with additional weights on each floor to meet the requirements of gravity and dynamic mass simulation [23]. The test frame was provided with a slab to represent the actual field condition and to incorporate the stiffening and strength offered by the slab. This also helped in placing the weight on the model for testing. Figure 2 reports the geometric and reinforcement details of the test frame. Further details about the test setup, instrumentation plan, loading protocols and scaling factors are described in Rizwan et al [22].

Table 3: Seismicity and structural data for standard occupancy SMRF structure in high seismic zone.

Property	Site Soil	Seismic Zone	C_V	I	R
Value	Type B	Zone 4	0.40	1.0	8.50

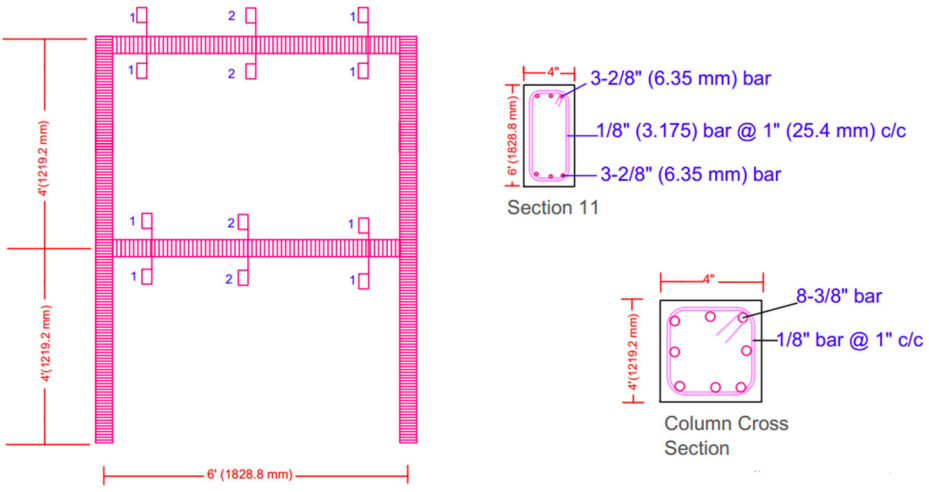

Figure 2: Geometric and reinforcement details of the 1:3 reduced scale frame for shake table testing.

Damages Observed in Deficient Test Frame

Shake-table tests were performed on the test frame by Rizwan et al. [22] using the 1994 Northridge earthquake ground motion. The ground motion was linearly scaled to multiple levels, which were input to the test frame for dynamic testing. Figure 3 reports the critical damages incurred by the test frame during the last test run, achieving the near collapse state. This model performed satisfactorily; resisting design base ground motions having peak horizontal acceleration equal to 0.40g without exceeding the code permissible story drift. Moreover, the test frame resisted ground motion with peak horizontal acceleration equal to 0.60g without collapse. However, the frame was found in a near collapse state. The present research made an attempt to assess the reliability of a low-cost technique in restoring, and possibly improving, the lateral resistance of this critically damaged frame. It is worth mentioning that, despite fulfilling the requirement (Equation 2) for beam-to-column flexure capacity ratio, the RC frame exhibited flexure hinging at the top of ground-story columns (Figure 3). This is partly due to the presence of a slab that contributed to the stiffness and strength of the beam, and also the material overstrength in the plastic hinge region of the beam that enhanced the flexure strength of the beam. This conforms to the recent observations regarding the overstrength in RC frames [24-25]. Moreover, the dynamic magnification also amplified the flexure demand at the top ends of the columns.

Damage at the Base of Ground-Story Column

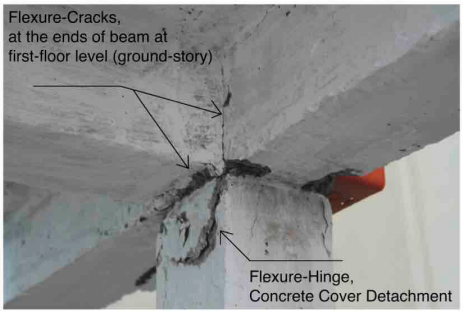

Damages Incurred in Beam/Column Members

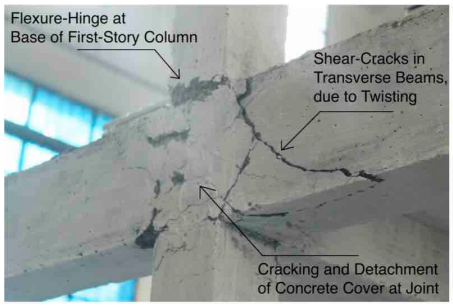

Beam-Column Connection at First-Floor Level

Beam-Column Connection at Second-Floor Level

Figure 3: Critical damages observed in the original RC test frame under extreme loading (Rizwan et al. [22]).

Strengthening Process

In the first phase of strengthening, the damaged frame was repositioned with the help of vertical steel posts and vertically lifting mechanical jacks, and it was further supported by means of external steel-tubular frame that contained the frame by preventing vertical movement and side-sway (Figure 4).

The damaged and crumbled concrete at connections was removed and replaced with high-strength new concrete. In particular, over the plastic hinge length at the ends of beams and columns i.e. length equal to $2h$ (h is the beam/column section depth) from the beam-column interface. The damaged cover concrete was removed by means of hammer and chisel while the core concrete was removed through drilling into concrete. Efforts were made not to damage the reinforcement of beam/column members. High-strength of concrete was achieved by adding silica fumes (10%) and superplasticizer (1%) to the normal concrete as a replacement of cement. A 3/8 inch (9.50 mm) down coarse aggregates were used in a mix proportion of 1:1:2 (cement: sand: aggregates) with water-to-cement ratio equal to 0.40. Standard concrete cylinders were prepared during the repair process of test model, which were cured for 28 days and tested for compressive strength. An average compressive strength approximately equal to 35 MPa was achieved for the new concrete. The bond between existing and new concrete was achieved by using epoxy mortar as a bonding agent applied at the interface.

It was desirable to allow the plastic hinges form in the beam/column members at distance from the beam-column interface (i.e. outside the previous plastic hinge length). Also, due to the insufficient development length of longitudinal beam bars and lesser than the required depth of the joint parallel to the beam longitudinal bars, joint shear hinge was developed in the original test frame [22]. The later required either strengthening of the joints (e.g. RC or steel jacketing or CFRP, etc.) or an intervention to reduce shear demands on joints. Therefore, fully fastened steel haunches were installed at the connections of the frame using post-installed anchors. This is expected to reduce shear demand on joint, allow beam-column members to deform inelastically under lateral loads and have the additional advantage of increasing lateral stiffness and strength of the frame. The design procedure described by Genesio [8] was used to design the steel haunches for the prototype of test frame. The geometrical and material properties of the preliminary designed haunches are contained in Table 4 while schematic views are reported in Figure 5. The geometric details are shown for the prototype frame, therefore, the dimensions were reduced by a scale factor of S_L = 3 for test frame. Haunches were installed below and above the first-floor beam while at the roof level a haunch was installed only below the beam.

Figure 4: Replacement of damaged concrete: (left) Damaged concrete removed at the connection; and (right) New high-strength concrete was used as a replacement.

Table 4: Geometric and material properties of the preliminary designed steel haunch following the design guidelines given in Genesio [8] for the prototype frame.

	Properties	Value
Haunch Details	Haunch diagonal (L_h)	1059 mm
	Projected length (L')	750 mm
	Haunch element angle (α)	45^0
	Elastic Modulus (Es)	200 GPa
	Haunch element cross-sectional area (A_d)	9720 mm^2
	Haunch element axial stiffness (K_d)	1836 kN/mm
Anchorage Details	Anchor type, mild steel rebar	Bonded Anchors
	Number of anchors (n)	6
	Yield strength (f_y)	414 MPa
	Effective depth (h_{ef})	180 mm
	Diameter (d_{nom})	24 mm
	Ultimate Strength (f_u)	550 MPa

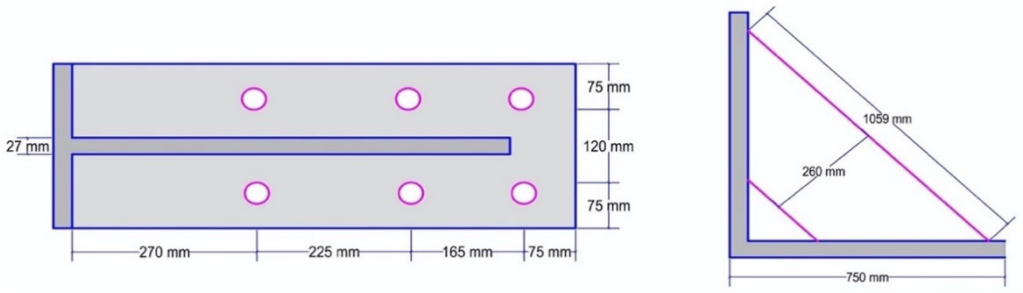

Figure 5: Schematic illustration of preliminary designed steel haunches: plan view (left) and side elevation (right) for the prototype frame.

The preliminary designed haunches should resist the maximum lateral force (V) that can develop in the frame, while responding elastically, which is calculated using Equation (3):

$$V = \Omega_R \times V_D \tag{3}$$

where Ω_R is the overstrength factor of strengthened RC frame. Current seismic codes (e.g. ASCE-7-16) suggest overstrength factor of 3.0 for SMRFs, but guidelines lack any recommendation for strengthened RC frames. In this research, the overstrength factor Ω_R will be determined through experimental quasi-static cyclic tests performed on retrofitted RC frame. The overstrength factor derived in this research is

expected to facilitate analysis and preliminary design of other similar structures.

QUASI-STATIC CYCLIC TESTS ON STRENGTHENED RC FRAME

Experimental Test Setup, Instrumentation and Lateral Loading Protocols

The strengthened frame was positioned for in-plane loading and secured to the strong floor through anchors (Figure 6). Only a single hydraulic actuator was available for applying lateral cyclic displacement, therefore, a vertical distribution beam was attached to the test frame by means of steel anchors to subject both the floors to lateral forces. A hydraulic actuator was attached to this distribution beam and positioned to distribute the lateral applied load in a proportion such that a 2/3rd load is transferred to the roof and 1/3rd is transferred to the first floor. This assumed force distribution is consistent with the vertical distribution of base shear over the height of the structure for fundamental mode, suggested in the absence of a more rigorous procedure [21]. The total lateral force was measured through a load cell mounted at the actuator. It is worth mentioning that the assumed invariant force distribution has limitation; when the structure undergoes inelastic behaviour, the stiffness at each floor changes disproportionally which alters the deflected shape of the structure, and consequently, the effective forces must change during lateral sway. However, in present research, experimental response of the frame is considered as a basis to validate/calibrate inelastic numerical model. This numerical model is then used in response history analysis for seismic performance assessment of the frame (discussed in the following sections).

Displacement transducers were installed at each floor of the test frame to measure the lateral displacement response of the frame (i.e. relative inelastic deformations and deflected shape of the frame under lateral loads), which is crucial for modelling the inelastic behaviour of frames under lateral load. A displacement transducer was installed also at the base to measure possible horizontal sliding of the test frame.

The loading history comprised of multiple cycles of displacements (Figure 7), having three cycles for each displacement level, which was prepared following the ACI ITG recommendations. The amplitude of the first three cycles does not exceed the 60 percent of the design displacement (i.e. story drift of 2.50%) and incremented such that the ratio of the maximum displacement of the subsequent cycles to the previous cycles remains between 1.25 to 1.50. The strengthened frame was tested progressively and was inspected for possible damages after three cycles of each displacement level.

Damages Observed in Strengthened RC Frame

The test frame did not exhibit any appreciable damage for lower drift demands (i.e. 0.40% and 0.50%) except the closing/opening of pre-existing distributed cracks in beam/column members. These were found in the beam/column members outside the plastic hinge region. Because, these distributed cracks were left unrepaired to economise and simplify the strengthening process. Flexure cracks were observed in the first-floor beam at the haunch location for a roof drift demand equal to 0.70%. This was followed by the appearance of a horizontal crack at the beam-haunch interface for roof drift equal to 1.0%. This aggravated after increasing roof drift demand to 1.50%, and then 2.0%. This indicates tension demand on haunches and the resulting slippage/pull out of post-installed anchors. The flexure cracks in the beam widened further. Additionally, flexure cracks were observed at the base of ground-story columns. Haunches installed below the first-floor beam fully detached due to concrete pry-out failure under the roof drift demand equal to 2.50%. The remaining haunches were still intact and the frame was able to deform up to roof drift equal to 3.50%. However, the model after this run was found in the near-collapse state. This was due to the likely concrete core crushing at the top and base of the ground-story columns. The observed damages of the model under significant runs are reported in Figure 8. Table 5 reports description of damages observed with increasing roof drift demand.

The application of haunches protected the joints from developing shear hinge and controlled the hierarchy of strength within the beam-column members. However, the hammering effect of haunches under compression developed localized damages in beam/column members at the haunch location (Figure 8). This weakens the internal microstructure of concrete, thus, allowing slippage of anchors and concrete pry-out failure. This fact limits the lateral deformation capacity of the frame under lateral load, which requires caution for application of the haunch retrofitting technique in seismic zones experiencing strong ground motions.

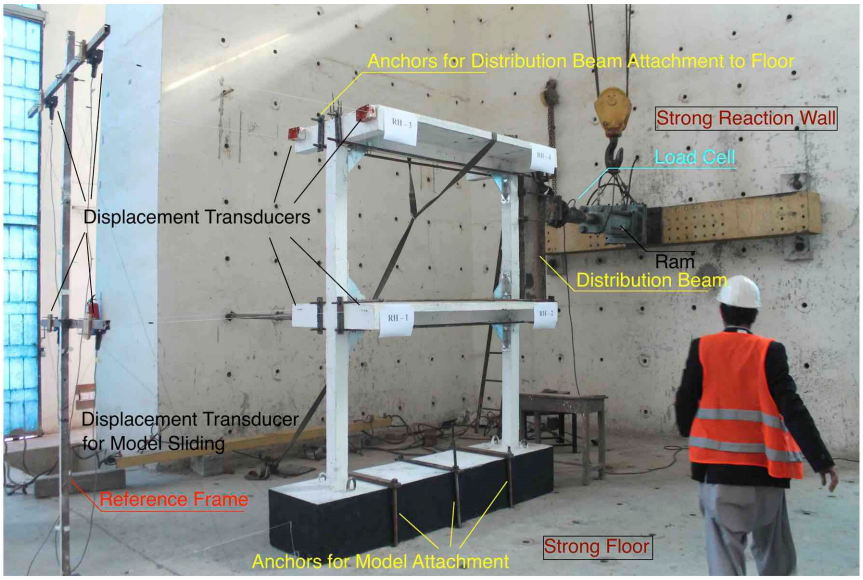

Figure 6: Test setup and instrumentation for quasi-static cyclic load tests on the frame.

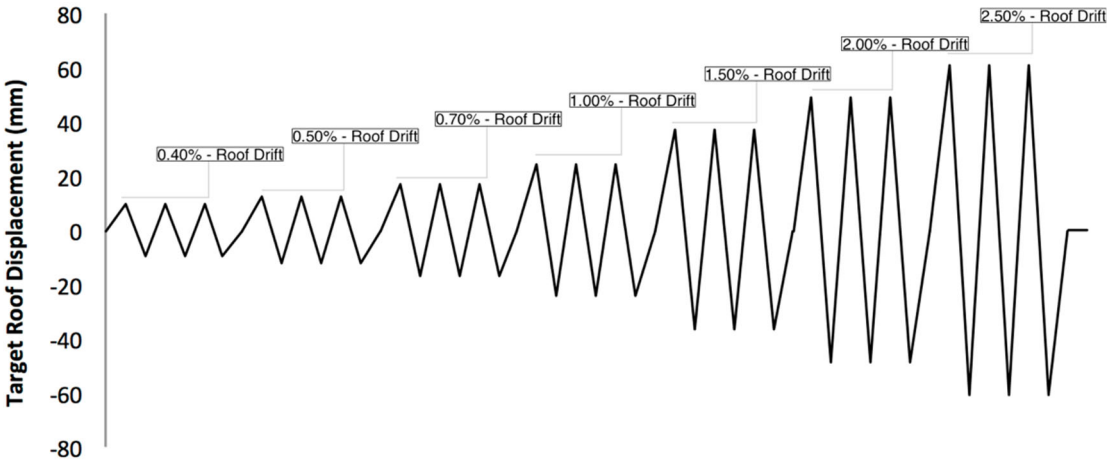

Figure 7: Roof displacement history for quasi-static cyclic load tests on frame.

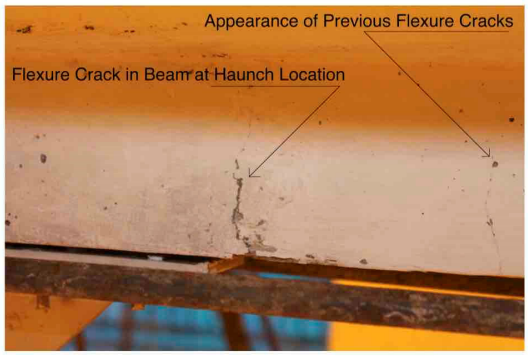

Slight Flexure Cracks in Beam on Ground Floor

Horizontal Crack at Haunch-Beam Interface

Significant Damages Observed in Model under 1.50% Roof Drift

Concrete Core Breakout of Anchorage on Ground Floor

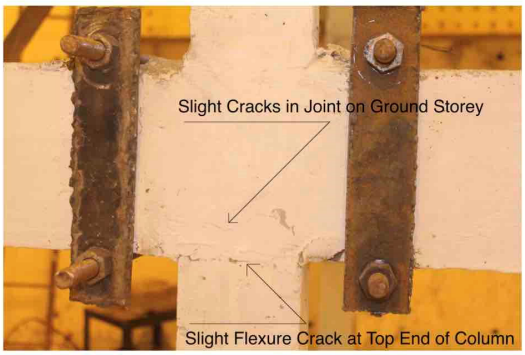

Slight Cracking in Joint and Column Top Ends

Significant Damages Observed in Model under 2.00% Roof Drift

Complete Detachment of Haunch on Ground Floor

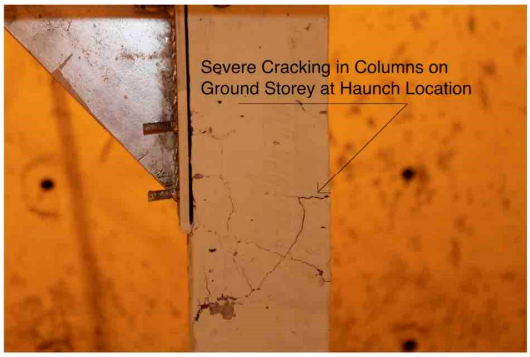

Severe Cracking in Columns at Haunch Location

Significant Damages Observed in Model under 3.50% Roof Drift

Figure 8: Damage evolution in the strengthened frame under simulated lateral loads.

Table 5: Description of damages observed in retrofitted frame with increasing roof drift demand.

S. No.	Roof Drift (%)	Observations
1	0.40	- Appearance of slight flexure cracks in beam on ground storey, mostly previous cracks which were only whitewashed. - This was also confirmed by the pinching behaviour of the force-displacement response of model.
2	0.50	- No further cracks were observed, except the opening & closing of pre-existing cracks.
3	0.70	- Appearance of flexure cracks in beam on ground floor at the location of haunch application (RH1 side).
4	1.00	- Appearance of horizontal cracks on ground storey at haunch-beam interface due to pull-out action in tension (RH2 side). - Slight cracks in column on ground storey at the location of haunch attaching bolts (RH2 side)
5	1.50	- Clearly visible opening & closing of horizontal crack at the haunch-beam interface on ground storey. - Significant flexure crack in beam at the haunch location on ground storey. - Slight flexure crack at the base of column on ground story (RH1 side) - Appearance of slight shear cracks in joint on ground storey.
6	2.00	- Further widening of flexure crack in beam at the haunch location on ground storey. - Significant flexure cracks at the base of columns on ground storey. - Slight flexure cracking at the top of column at the location of haunch and also at the top ends. - Slight flexure cracks at the base of column on first storey. - Cracking at interface of haunch-beam on first storey (RH3 side).
7	2.50	- Further widening of flexure crack and few spalling observed in beam at the location of haunch application on ground storey. - Further widening of flexure cracks at the base of columns on ground storey. - Detachment of haunch due to pull-out and removal of chunk (pry-out) of concrete from beam at haunch location.
8	3.50	- Severe flexure cracks at the base of columns on ground storey, likely to cause cover and core crushing. - Full detachment of haunches at the ground storey applied below the beam and a clear horizontal crack at the haunch-beam interface for haunches applied above the beam. - Significant flexure and shear cracks in columns on ground storey at the location of haunch application.

RESPONSE OF STRENGTHENED RC FRAME UNDER CYCLIC LATERAL LOADS

Hysteretic Damping of Strengthened RC Frame

Structural damping is a key parameter in controlling vibrations of a structure responding inelastically when excited by ground motions. It is quantified in terms of damping ratio (i.e. the ratio of damping in the structure to the critical damping), which is a measure of the energy dissipation potential of the structure. A higher value of damping in a structure indicates better seismic performance; as it reduces lateral deformation demands, and thereby, limits damage in structure subjected to ground motions.

The applied roof displacement was multiplied by a scale factor $S_L = 3$ and the measured force was multiplied by a scale factor $S_L^2 = 3^2 = 9$ to convert the model response quantities to prototype [22]. Figure 9 reports the hysteretic response of the retrofitted frame, which was obtained by correlating the base shear force with the applied roof drift. The data was plotted up to maximum roof drift equal to 2.50%, which is the maximum permissible drift under design basis ground motions. For calculating the hysteretic damping of the frame, the concept of dissipated energy in a cycle to input energy has been used, and quantified using Equation (4) proposed by Jacobsen [26] for inelastic single degree of freedom system:

$$\xi_{hyst} = \frac{E_{diss}}{2\pi E_{in}} \tag{4}$$

where ξ_{hyst} is the hysteretic damping of system under a given cycle, E_{diss} is the energy dissipated by the system for a cyclic displacement demand and E_{in} is the input energy to the system. E_{diss} was measured by calculating the total area under the curve of the hysteretic cycle using the trapezoidal rule. E_{in} was computed for each cycle by calculating the area under the curve for the equivalent elastic response of the system. The variation of hysteretic damping with damage progression in the frame

was studied by correlating the computed hysteretic damping with the roof drift demand (Figure 9). The first three cycles were not considered for computation of damping due to the skewed response of the frame. A maximum hysteretic damping of 11% and an average of 9.50% were obtained. Despite the pinching behaviour, the test model exhibited significant hysteretic damping, which is due to the increase in post-yield stiffness and lateral strength of the frame.

The simplified static displacement-based seismic design procedure combines the hysteretic and elastic damping to idealize the total equivalent viscous damping of an inelastic system [27]. Considering a 5% elastic damping, the tested frame gives total viscous damping equal to 16% for the design level deformation capacity (i.e. 2.50% roof drift). As it is unlikely for structures responding inelastically during ground motions to develop symmetric force-displacement hysteretic response similar to the response obtained through quasi-static cyclic tests, Priestley et al. [27] recommended correction factors to the hysteretic curve area-based equivalent viscus damping. A correction factor approximately equal to 0.90 is suggested for RC structures with Takeda thin hysteretic rule. Reducing the hysteretic damping (0.9 x 11) and combining this with the elastic damping gives total viscous damping approximately equal to 15%, which is still encouraging for a recycled RC frame. This value is in close agreement with the viscous damping suggested for the seismic design of RC frame structures [27].

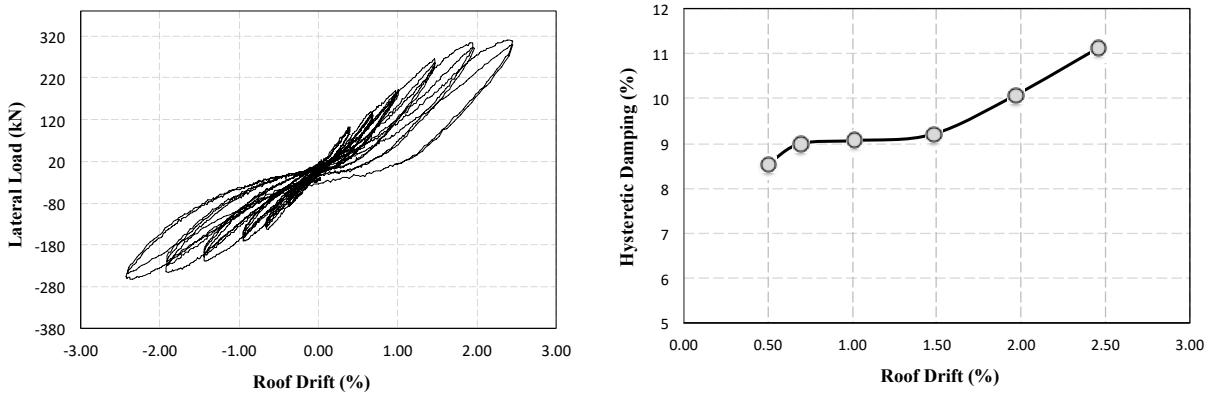

Figure 9: Force-deformation hysteretic response of prototype of the strengthened frame (left) and the corresponding hysteretic damping of the strengthened frame (right).

Lateral Resistance – Displacement Curve of Strengthened RC Frame

The lateral load-displacement response curve is an essential plot to calculate a number of crucial parameters like initial lateral stiffness of structure, peak strength, ductility, and stiffness/strength deterioration. Moreover, this plot is used as a basis to develop performance levels for performance-based design of structures [28].

The peak roof displacement demand for push/pull direction were identified for which the corresponding peak lateral resistance was obtained. The mean lateral resistance was correlated with the relative roof displacement to develop the capacity curve for the strengthened frame (Figure 10). This was compared with the capacity curve derived earlier for the original frame (Figure 10), obtained from [22]. The strengthened frame exhibited an increase in initial stiffness, lateral resistance, and post-yield stiffness under lateral load. This is advantageous for minimising structural/non-structural damages during strong ground motions; as a structure with a higher post-yield stiffness will result in a relatively lower residual displacement demand in comparison to structures with no or lower post-yield stiffness. However, the strengthening technique did not restore the deformation capacity of the damaged frame and reached the near-collapse state at roof drift demand equal to 3.50%. Nevertheless, it will be evident in the following sections that the higher post-yield stiffness controlled the deformation demand on structure. The deformation demand did not exceed the collapse limit state in majority of the ground motions corresponding to the maximum considered earthquakes. The strengthened frame resisted a maximum lateral force of 290 kN which is 52.63 % higher than the later force = 190 kN resisted by the original frame. The strengthened frame gives an overstrength factor Ω_R (i.e. the ratio of peak resistance to the design base shear) equal to 4.14. This is approximately 1.52 times the overstrength factor of the original RC frame, that represents the effectiveness factor of retrofitting scheme [29].

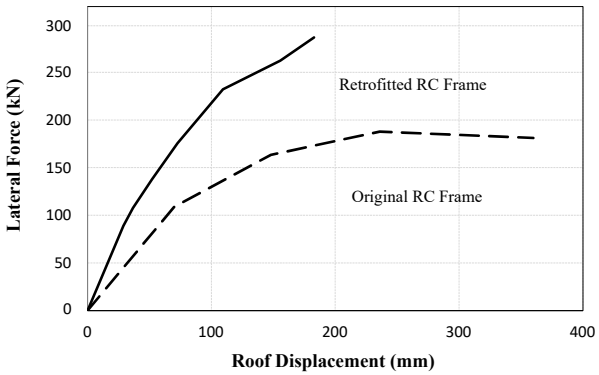

Figure 10: The lateral resistance-displacement capacity curve of a prototype of the strengthened frame. The capacity curve of original frame tested by Rizwan et al. [22] is also shown.

Performance Levels of Strengthened RC Frame

Performance levels were developed for the strengthened frames following the FEMA-356 guidelines [28]. This comprised of Immediate Occupancy (IO), Life Safety (LS), and Collapse Prevention (CP) limit states. The deformation limits were expressed in terms of roof drift and story drift while the strength limits were expressed in terms of base shear coefficient (BSC) i.e. dividing the lateral force by the seismic weight of the frame. Although the strengthened frame was able to deform up to roof drift equal to 3.50 %, the frame was extensively damaged at the roof drift demand equal to 2.50%. Thus, the later was considered as the drift capacity corresponding to the CP limit state. The roof drift corresponding to the LS limit state was

considered equal to 75% of the drift capacity corresponding to the CP limit state. The drift capacity for the IO limit state was approximated as equal to 70% of the drift capacity corresponding to the LS limit state. The corresponding BSCs were obtained from the capacity curve through linear interpolation. Table 6 and Figure 11 report performance levels developed for the strengthened RC frames.

Figure 12 reports the peak relative displacement and the corresponding peak story drift response of frame observed under each test run, which indicates the story drift at ground-story is higher than the roof drift. This is due to the disproportionate damages that occurred at the ground and first stories under lateral load. A linear trend was observed between the roof drift and story drift at the ground story (Figure 12c), the story drift is found to be 30% higher than the roof drift. The corresponding story drift for each of the performance levels is reported in Table 6.

Although the frame reached the near-collapse state at a roof drift of 2.50%, the frame achieved story drift equal to 3.20%. It is worth mentioning that in seismic design codes, the deformation limit is based on the story drift rather than the roof drift. For low-rise RC frames, codes permit story drift up to 2.50% under design level forces. The present tests confirm the improved seismic behaviour of retrofitted frame; as the frame achieved story drift capacity equal to 2.50% corresponding to the life safety limit state, which is in agreement with the permissible story drift for a code-conforming structure.

Table 6: Performance levels developed for strengthened RC frame.

	Performance Levels		
Parameters	**Immediate Occupancy**	**Life Safety**	**Collapse Prevention**
Roof Drift (%)	1.30	1.88	2.50
Story Drift (%)	1.68	2.50	3.20
BSC*	0.33	0.40	0.45
Damages	Significant flexure cracks develop in the beam at the first-floor level.	Existing flexure cracks in beams widen further. Steel haunches below the first-floor beam de-bond from the beam. The flexure cracks initiate at the base of ground-story columns.	Existing flexure cracks in the beam aggravate. Steel haunches below the first-floor beam completely detach from the beam. Cover crushing at the base of the ground-story columns. Significant flexure and shear cracks were also observed at top of the ground story columns at the haunch location.

*BSC (Base Shear Coefficient), calculated by normalizing base shear force over the weight of the structure.

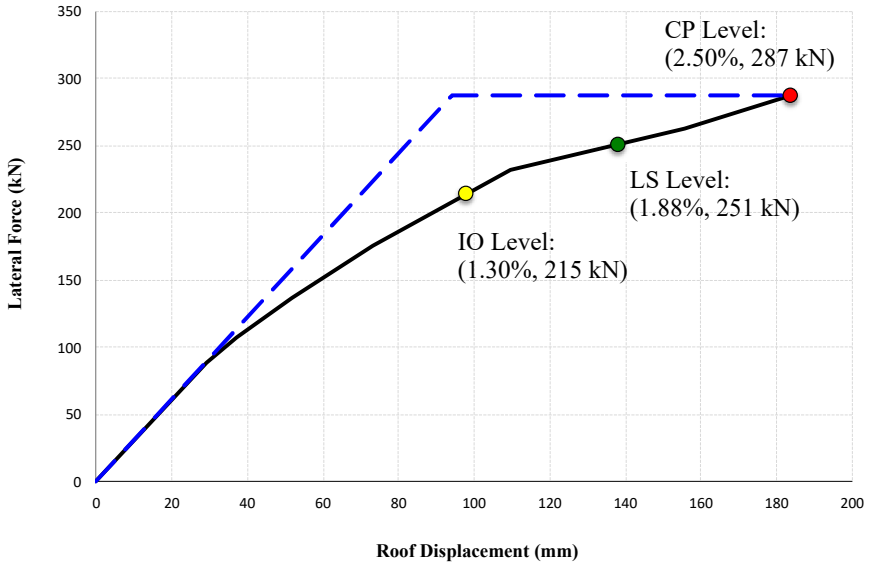

Figure 11: Performance levels on the force-displacement capacity curve of the strengthened RC frame. (The roof drifts and the corresponding lateral forces are shown in brackets)

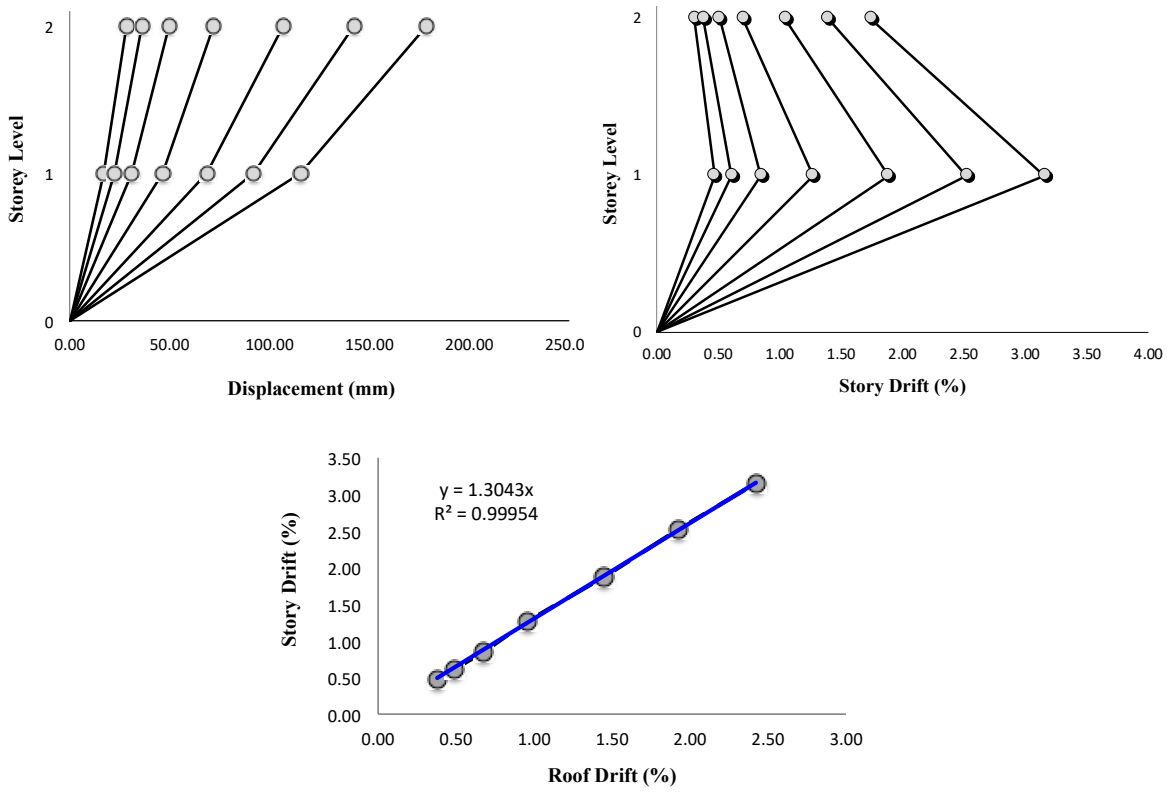

Figure 12: Lateral displacement response of rehabilitated RC frame: (top left) relative displacement profile; (top right) story drift profile; and (bottom) relationship between roof drift and story drift at the ground story.

RESPONSE HISTORY ANALYSIS OF STRENGTHENED RC FRAME

Calibration of Finite Element Based Numerical Models for Strengthened Frame

Majority of the structural analysis programs are intended for analysis and design of new structures. Therefore, the element modelling techniques and material models are those for the code conforming structures. The application of such analysis program for modelling of existing/retrofitting structures is likely to underestimate the response displacement of frames, which is a key parameter for seismic performance assessment of the structure for an ensemble of ground motions. Therefore, it is essential to test/validate and calibrate the numerical model before performing static or dynamic analysis.

A representative numerical model was prepared for the prototype of test frame in the finite element program SeismoStruct (Figure 13). The beam/column members were modelled using the fiber-section based bending element with distributed plasticity. This uses the force-based formulation to simulate both the geometric and material nonlinearities. Each fiber at the section is assigned with the associated uniaxial stress-strain relationships for unconfined and confined concrete and reinforcing steel bars.

The experimental model exhibited closing/opening of existing distributed cracks in beam/members outside the plastic hinge region under later load. This adds flexibility to the member and results in pinching in the lateral resistance-displacement hysteretic response of the frame (Figure 9). For this purpose, a moment-rotational link element was introduced at the beam-ends to simulate an inelastic extension of longitudinal steel bars and fixed-end rotation. Although, a more realistic force-deformation backbone envelope curve may be used to model the beam fixed-end rotation [30], a rather simplified moment-rotation hysteretic response (modified Takeda hysteresis) was used in the present study to simulate this phenomenon [31], which is simple and reasonable for global assessment.

In case of haunches attached to the beam/column members by means of external anchors, the numerical model included rigid links between the haunches and beam/column members [7]. However, in case of post-installed direct anchors, the haunches cause hammering effect on the beam/column members, as evident during experimental quasi-static cyclic tests (Figure 8). Therefore, the steel haunches in present case were modelled by directly attaching a diagonal element (haunch element) to the beam/column members. The haunch elements were modelled as inelastic truss elements with fiber-section to simulate the tension/compression behaviour of haunches. The anchors' slippage/pull-out can be modelled directly attaching springs at the diagonal element and beam/column elements intersection [10]. This needs to be provisioned with appropriate nonlinear force-deformation relationships to simulate slippage/pull-out response [32]. Alternatively, strain limits may be imposed on the diagonal elements, whereby the contribution from the element may be discarded i.e. simulating the haunch pull-out. Since the pull-out may occur before the haunch element yielding, it needs to be defined based on experimental calibrations. For this purpose, the numerical model was subjected to floor forces measured during the imposed lateral roof displacement corresponding to the 2.50% roof drift. Tension strain equal to 0.0003 was found reasonable to define limiting strain for haunch pull-out.

Additionally, an elastic numerical model was prepared for the considered strengthened frame in the SAP2000 program, including the steel haunches. The frame was analyzed for a lateral load $V = \Omega_R \times V_D =$ 290 kN, where Ω_R was obtained experimentally and approximated to 4.14. The maximum tension force developed in steel haunch at the first-floor level was equal to 544 kN. For haunch attached to beam/column members with six anchors, this gives approximately 64 kN shear and pull-out load demand on a single anchor. Such analysis will facilitate the preliminary design of anchors.

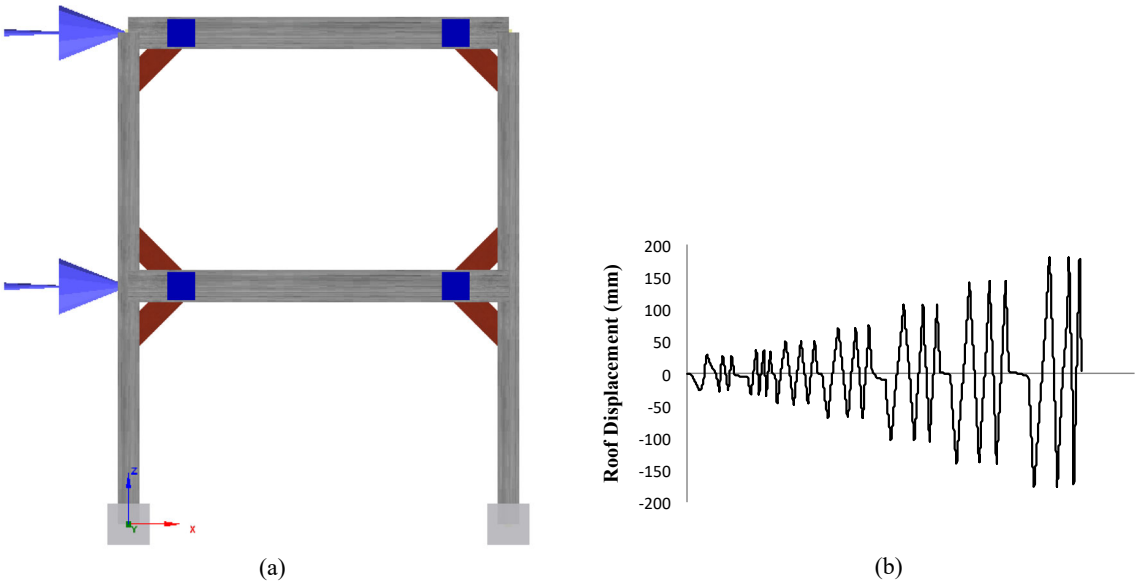

(a) (b)

Figure 13: Calibration of numerical model: (a) inelastic numerical model prepared in SeismoStruct; and (b) actual roof displacement loading.

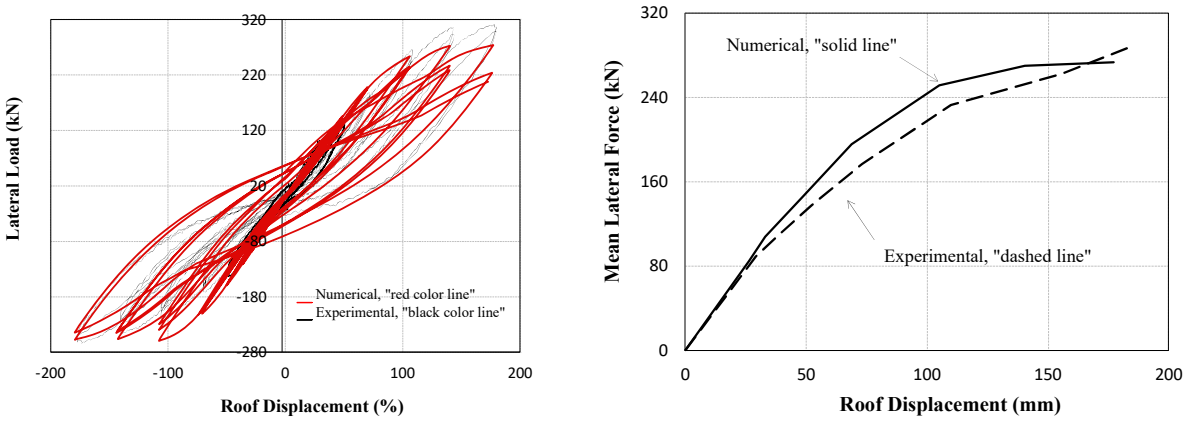

(a) (b)

Figure 14: Test and validation of the numerical model: (a) comparison of lateral resistance-displacement hysteretic response; and (b) lateral resistance-displacement capacity curves.

Moreover, the inelastic numerical model was subjected to the actual roof displacement history applied to the test frame (Figure 13b). The lateral floor displacements were applied in such proportion to simulate the inelastic deflected shape of the test model. Therefore, displacement multipliers were considered as 1.0 and 0.60 for roof and first-floor levels respectively. It is worth mentioning that 2.50% roof drift demand represents the CP limit states of the strengthened frame (Table 6), therefore, the anchor pull-out during analysis was ignored. Figure 14a reports the resistance-displacement hysteretic response of the numerical model along with the experimentally measured response. Figure 14b reports the numerically predicted resistance-displacement peak envelope curve along with the mean experimental envelope curve. The numerical model behaved reasonably in simulating the initial and post-yield stiffness, lateral strength, and lateral resistance-displacement hysteretic response of the strengthened RC frame.

Response History Analysis of Two-Story Frame for DBE and MCE

The modern performance-based assessment methods require seismic analyses of structures for design basis ground motions and ground motions corresponding to maximum considered earthquakes. It is hence essential to confirm that the retrofitting technique meets the objectives of seismic design i.e. the structure should not exceed the life safety limit state under design basis ground motions and it should not exceed the collapse prevention limit state when subjected to ground motions corresponding to maximum considered earthquakes.

Before the response history analysis, the calibrated finite element model was studied through the Eigenvalue analysis procedure to obtain the fundamental vibration period of the model, which was found equal to 0.57 sec for the first mode of vibration. The model was assigned with tangent stiffness proportional elastic damping equal to 2%, as found reasonable for seismic analysis of finite element model using fiber-section based elements for beam/column members [18,33].

A set of seven ground motions were obtained from the PEER strong motions database for active shallow crustal earthquakes having reverse/reverse-oblique fault mechanisms. The selected ground motions have moment magnitude varying from 6.50 to 7.01. These were recorded in the intermediate-fault regions with source-to-site distance from 12.38 km to 28.90 km. The selected ground motions were scaled and matched to the design spectrum through the wavelet-based procedure using the SeismoMatch program. Figure 15 reports the mean response spectrum developed for the selected scaled/matched ground motions and Table 7 reports the details of the selected ground motions.

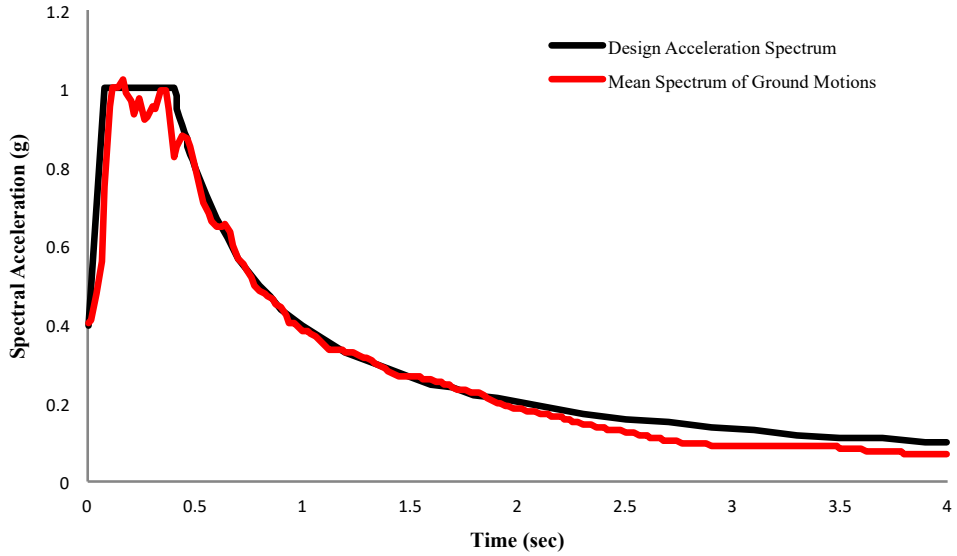

Figure 15: Mean acceleration spectrum of selected scaled/matched accelerograms.

Table 7: Details of the scaled ground motions used for response history analysis.

S. No.	Event	Year	Station	Mw	R_{jb}	SA(T_1)
1	Cape Mendocino	1992	Loleta Fire Station	7.01	23.46	0.62g
2	Northridge	1994	Sunland - Mt Gleason Ave	6.69	12.38	0.71g
3	San Fernando	1971	Santa Felita Dam (Outlet)	6.61	24.69	0.55g
4	Loma Prieta	1989	Coyote Lake Dam – Southwest abutment	6.93	19.97	0.66g
5	San Simeon	2003	San Antonio Dam - Toe	6.52	16.17	0.75g
6	Niigata-Chuetsu	2007	Joetsu Ogataku	6.80	16.77	0.68g
7	Iwate	2008	Semine Kurihara City	6.90	28.90	0.75g

The numerical model was analysed through the response history analysis procedure to assess the performance of the strengthened RC frame under design base earthquake (DBE). Moreover, the ground motions were linearly scaled by a scale factor of 3/2 (=1.50) to approximate the ground motions corresponding to the maximum considered earthquake (MCE). This approximation considers that the amplitude of acceleration of ground motions for MCE is equal to 3/2 times the amplitude of acceleration of ground motions corresponding to DBE, similar to the consideration adopted in the ASCE-7-16 [34] for conversion of MCE ground motions to DBE. The average story drift demands are reported in Figure 16 for DBE and MCE ground motions. The average drift demand under DBE is less than LS while the average drift demand under MCE is less than CP. This good behaviour of the model is due to the installation of steel haunches that increased the lateral stiffness and resistance of the model, benefiting the frame to control deformation demand. The RHA of the model have revealed that although the model exceeded the IO level under DBE ground motions, it didn't exceed the LS level, except the ground motion of San Simeon 2003 earthquake that deformed the ground-story beyond the LS level. Likewise, the model exceeded the LS level but didn't exceed the CP level under MCE ground motions, except the ground motions of the San Simeon 2003 earthquake. Despite the fact that the retrofitted frame exhibited pinching behaviour in the force-displacement hysteretic response, the frame still performed better due to the high stiffness and strength after retrofitting. However, it is worth mentioning that this good behaviour is also subjective and depends on the characteristics of the selected ground motions and the scaling procedure. For example, the same frame may perform differently in case of ground motions of near-fault regions or ground motions with site amplification in the proximity of frame fundamental mode. In the later cases, the performance of structure has to be assessed as per the region specific seismicity, and if required, alternative retrofitting technique may be adopted.

PERFORMANCE ASSESSMENT OF STRENGTHENED MULTI-STORY RC FRAMES

Design of Steel Haunches for Strengthening of Multi-Story RC Frames

The strengthening technique was extended to multi-story RC frame to evaluate the efficacy of the technique, and the simplified design procedure. An RC frame having five stories was considered, which is located in a high seismic hazard zone on rock site "Type B" soil. Figure 17 shows the geometric and

reinforcement details of the considered five-story RC frame. The frame is considered having material properties similar to that of the two-story frame (Table 1). The total seismic weight of the frame is 1588 kN. For strengthening, the design level base shear force of the frame was calculated using Equation (1) that gives V_D = 90 kN. This was increased using the overstrength factor (using Equation 3) to obtain the peak lateral load (V) for seismic analysis and preliminary design of steel haunches.

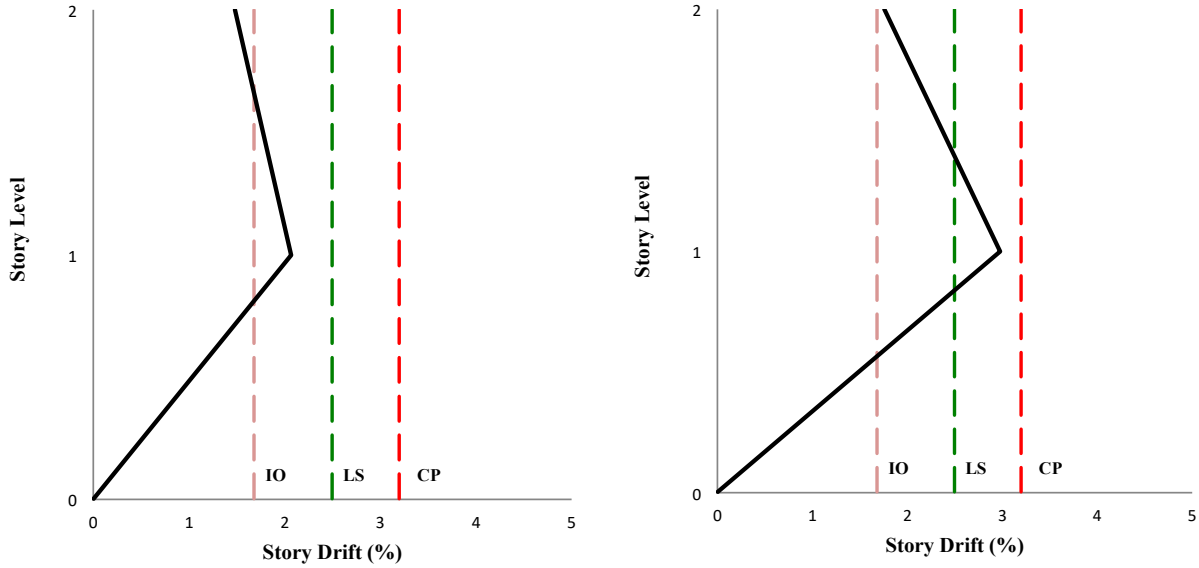

(Average of the ground motions for DBE) (Average of the ground motions for MCE)

Figure 16: Story drift demands (average) of strengthened two-story RC frame under DBE and MCE.

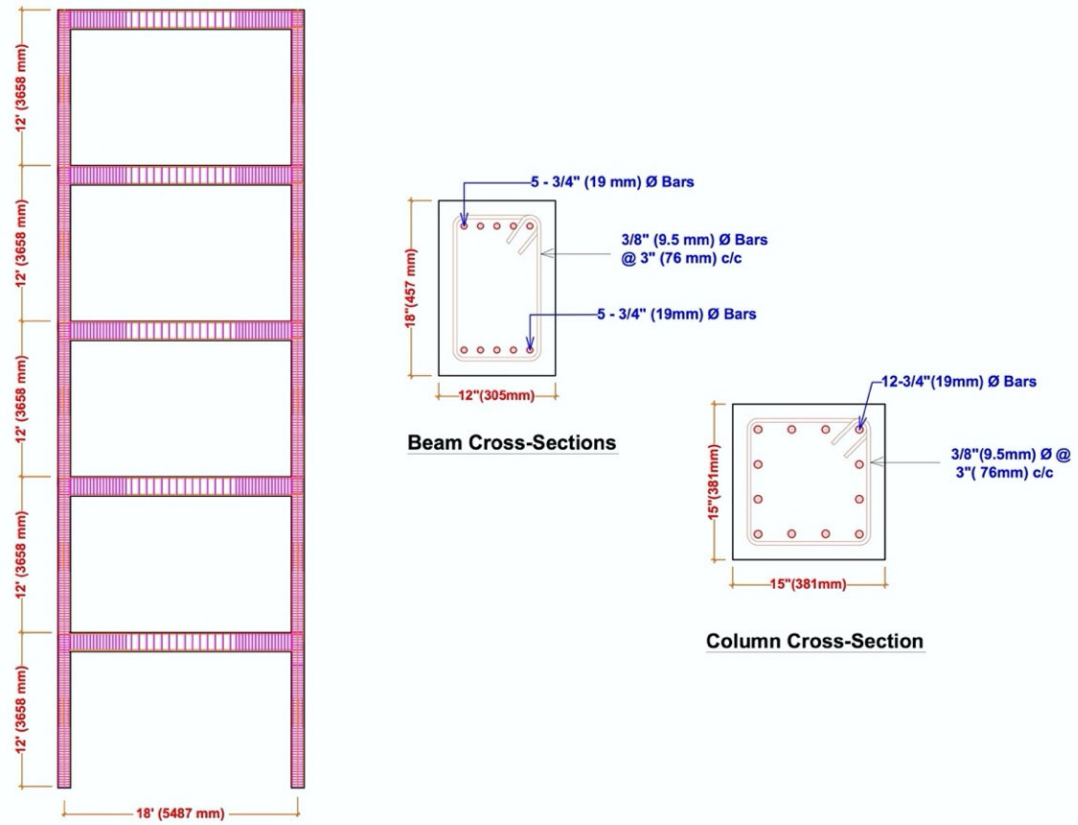

Figure 17: Geometric and reinforcement details of the five-story RC frame.

The experimental test performed on a two-story frame gave an overstrength factor Ω_R equal to 4.14, which was approximated to 4.0 for analysis and preliminary design of steel haunches for the considered five-story RC frame. For the preliminary design of steel haunches, the same geometric and material properties (i.e. given in Table 4 and shown in Figure 5) were considered. Response history analysis performed on multi-stories RC frames retrofitted with eccentric steel braces has revealed a non-uniform story drift demand, with the trend to develop maximum demands in middle stories [35]. Therefore, the beam-column connection at the second-floor level was analyzed, as this may experience the largest seismic demands. The haunch experienced a tension force of 593 kN, this gives anchor pull-out force of 70 kN using six anchors for attaching the haunch

plate to beam/column members. This gives a demand-to-capacity ratio equal to 1.10. However, it is worth to mention that this level of force will develop under the MCE level ground motions, which is very rare, and it is expected that the anchor pull-out force will be less under DBE level ground motions. Moreover, the anchor pull-out force for the remaining haunches was less. Therefore, the designer may consider this acceptable at the preliminary design stage, which will be verified through response history analysis for both DBE and MCE level ground motions. Any revision if warranted by the RHA shall consider revising the dimensions of steel haunches.

Nonlinear Static Pushover Analysis of Strengthened RC Frame

The considered five-story strengthened RC frame was modelled in the SeismoStruct program for nonlinear static pushover analysis. Initially, Eigenvalue analysis was performed to obtain the fundamental vibration period, which is equal to 1.03 sec, and the floor deformation of the model under the first mode of vibration; starting from roof to first-floor level, equal to [1.0 0.90 0.72 0.49, 0.22]. The floor displacements were defined at each floor level while the structure was pushed laterally till the CP level reached at the first-story level. Figure 18 (a) reports the inelastic deflected shapes when the story drift demand under lateral loads attained the LS and CP levels, respectively, for vibration in mode 1. Figure 18(b) reports the single anchor pull-out force for haunches under tension i.e. haunches below the beam at left-end [Level-1L, Level-2L, Level-3L, Level-4L, Level-5L,] and haunches above the beam at right-end [Level-1R, Level-2R, Level-3R, Level-4R]. The anchor pull-out forces both at LS and CP levels are less than the experimentally obtained pull-out capacity of anchor (64 kN), except the anchor force at the second-floor level (i.e. Level-2L) at the CP level, which is slightly higher than the capacity. However, this may happen under the ground motions corresponding to MCE, and only at one location, therefore, the inelastic pushover analysis suggests the preliminary design scheme is adequate and optimum for the considered frame.

Response History Analyses of Strengthened RC Frame

The inelastic model was also analyzed through response history analysis for both DBE and MCE ground motions. Figure 19 reports the average story drift demands under the DBE and MCE ground motions. Likewise, the five-story RC frame, although exceeded the story drift corresponding to the IO level, it did not exceed the story drift corresponding to the LS level under DBE ground motions. Similarly, the frame although exceeded story drift corresponding to LS level but it did not exceed the story drift corresponding to the CP level under the MCE ground motions. The steel haunches proved to be effective also for strengthening of mid-rise RC frames. This also confirms the efficacy of the simplified design approach and the proposed overstrength Ω_R equal to 4.0 for the preliminary design of steel haunches for strengthening RC frames.

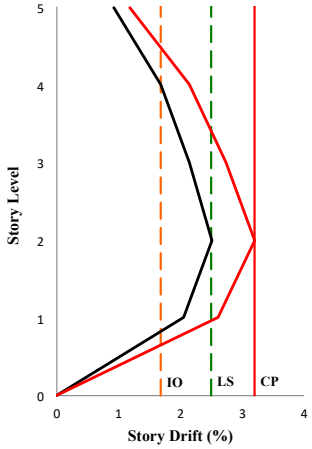

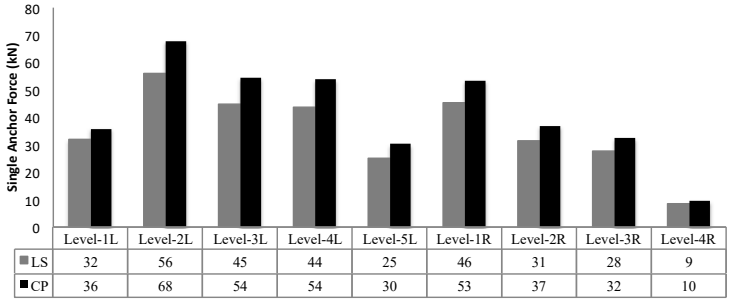

	Level-1L	Level-2L	Level-3L	Level-4L	Level-5L	Level-1R	Level-2R	Level-3R	Level-4R
LS	32	56	45	44	25	46	31	28	9
CP	36	68	54	54	30	53	37	32	10

Figure 18: Response under nonlinear static pushover analysis; (left) story drift demand and, (right) the corresponding force in the single anchor of tension loaded steel haunches.

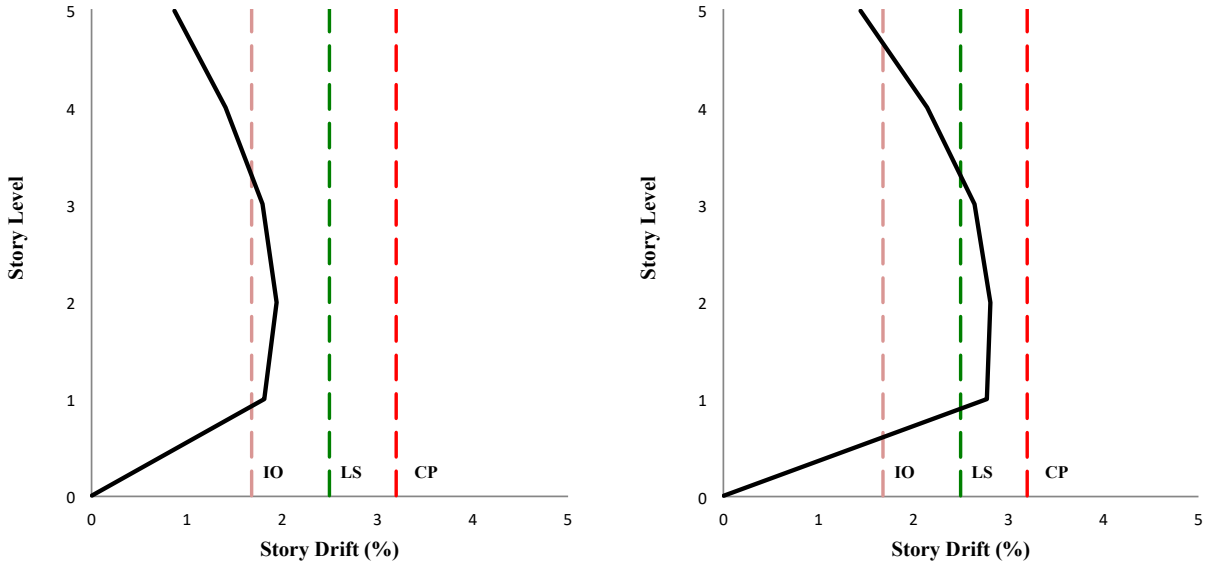

Figure 19: Story drift demands (average) of rehabilitated five-story RC frame under DBE (left) and MCE (right).

As mentioned earlier, the improved seismic performance is attributed to the increase in stiffness and strength of frame due to the installation of steel haunches at connections. Both the low-rise and mid-rise frames behaved similarly under a set of ground motions. Despite the increase in number of stories, the overstrength factor Ω_R = 4.0, selected based on the quasi-static cyclic tests on the two-story frame, seems reasonable for the seismic analysis and design of steel haunches and anchors for both low-rise and mid-rise frames.

The selected technique and the simplified design procedure seems to be conservative; having significant margin between the average demands and capacity. But this seems beneficial for field application, as the numerical model is a simplified idealization of the actual structure and it is always challenging to reproduce the exact material properties in the field.

CONCLUSIONS

The following are concluded based on the experimental and numerical studies performed on strengthened reinforced concrete moment-resisting frames:

High-strength of concrete have compressive strength equal to 5000 psi (35 MPa) may be achieved by adding silica fume (10% of cement) and superplasticizer (1% of cement) to normal concrete with a mix proportion of 1:1.0:2.0 (cement: sand: aggregate) with water-to-cement ratio equal to 0.40. Average hysteretic damping of 9.50 % was obtained for the strengthened RC frame, which increased up to 11 % at the roof drift demand equal to 2.50 %.

The strengthened frame was able to deform up to maximum story drift equal to 3.20%. The strengthened RC frame resisted a maximum lateral force of 290 kN which is 52.63% higher than the later force equal to 190 kN resisted by the original frame. The strengthened RC frame gives an overstrength factor Ω_R equal to 4.14. This is 1.52 times the overstrength factor of the original RC frame. The overstrength factor Ω_R = 4.0 may be considered for analysis and preliminary design of the strengthened RC frame. Performance levels were developed for the strengthened frame as per the FEMA 356 guidelines; suggesting roof drifts equal to 1.30 %, 1.88 % and 2.50 % corresponding to the immediate occupancy (IO), life safety (LS) and collapse prevention (CP) limit states respectively. The corresponding story drifts of 1.68 %, 2.50 %, and 3.20 % were obtained for the IO, LS, and CP limit states respectively.

Parametric analysis performed on conventional and calibrated numerical model confirmed the beneficial role of link element in simulating the pinching behaviour of lateral resistance-displacement hysteretic response of the strengthened frame. Response history analysis has revealed that the strengthened five-story RC frame, although exceeded the story drift corresponding to the IO level, did not exceed the story drift corresponding to the LS level under DBE ground motions. Similarly, the frame although exceeded story drift corresponding to LS level but it did not exceed the story drift corresponding to the CP level under the MCE ground motions. Thus, the response history analysis also confirms the adequacy of the preliminary design of steel haunches and the proposed overstrength factor Ω_R equal to 4.0 for lateral load analysis and preliminary design of steel haunches.

Both the low-rise and mid-rise retrofitted frames performed almost similarly under a set of ground motions, indicating the appropriateness of overstrength factor Ω_R = 4.0 for analysis and design of steel haunches and anchors for both low-rise and mid-rise frames. The present research described only a single specimen due to limited resources. The extension of the research to more specimens can generalize the findings presented herein, the retrofitting scheme and the simplified design procedure.

ACKNOWLEDGMENT

The authors are grateful to the board of advanced studies and research (BOASAR) of UET Peshawar for partially supporting the experimental part of the research. The anonymous reviewers are thanked for suggesting improvements in the manuscript.

REFERENCES

1 Engindeniz M, Kahn LF and Zureick A (2006). "Repair and strengthening of reinforced concrete beam-column joints: state of the art". *ACI Structural Journal*, **102**(2): 187-197. https://www.concrete.org/publications/internationalconcreteabstractsportal/m/details/id/14269

2 Tsonos AG (1999). "Lateral load response of strengthened RC beam-to-column joint". *ACI Structural Journal*, **96**(1): 46-56. https://www.concrete.org/publications/internationalconcreteabstractsportal/m/details/id/595

3 Dhakal RP, Pan TC and Tsai KC (2003). "*Enhancement of beam-column joint by RC jacketing*". Report-16 for the Civil Engineering Research, Nanyang Technological University, Singapore, 03pp. http://hdl.handle.net/10092/4198

4 Beydokhty EZ and Shariatmadar H (2016). "Behavior of damaged exterior RC beam-column joints strengthened by CFRP composites". *Latin American Journal of Solids and Structures*, **13**(5): 880-896. http://dx.doi.org/10.1590/1679-78252258

5 Pampanin S and Christopoulos C (2003). "Non-invasive retrofit of existing RC frames designed for gravity loads only". *Proceedings of the FIB Symposium on Concrete Structure in Seismic Regions*, May 6-8, Athens, Greece, 12pp. https://core.ac.uk/download/pdf/35457474.pdf

6 Chen TH (2006). "*Development of a low-invasive seismic retrofit solution for under-designed frame systems based on a metallic haunch*". Master Thesis, Department of Civil Engineering, University of Canterbury, Christchurch, New Zealand.

7 Pampanin S, Christopoulos C and Chen TH (2006). "Development and validation of a metallic haunch seismic retrofit solution for existing under-designed RC frame buildings". *Earthquake Engineering and Structural Dynamics*, **35**(14): 1739-1766. https://doi.org/10.1002/eqe.600

8 Genesio G (2012). "*Seismic assessment of RC exterior beam-column joints and retrofit with haunches using post-installed anchors*". PhD Dissertation, Stuttgart University, Germany, 311pp.

9 Sharma A (2013). "*Seismic behavior and retrofitting of RC frame structures with emphasis on beam-column joints – Experiments and numerical modeling*". PhD Dissertation, Stuttgart University, Germany, 391pp.

10 Sharma A, Reddy GR, Eligehausen R, Genesio G and Pampanin S (2014). "Seismic response of reinforced concrete frames with haunch retrofit solution". *ACI Structural Journal*, **111**(3): 673-684. https://www.concrete.org/publications/internationalconcreteabstractsportal.aspx?m=details&ID=51686625

11 Khalili A, Kheyroddin A, Farahani A and Sharbatdar MK (2015). "Nonlinear behavior of RC frames strengthened with steel curb and prop". *Scientia Iranica – Transactions A: Civil Engineering*, **22**(5): 1712-1722. http://scientiairanica.sharif.edu/article_1991.html

12 Kheyroddin A, Khalili A, Emami E and Sharbatdar MK (2016). "An innovative experimental method to upgrade performance of external weak RC joints using fused steel

prop plus sheets". *Steel and Composite Structures*, **21**(2): 443-460. http://dx.doi.org/10.12989/scs.2016.21.2.443

13 Kanchanadevi A and Ramanjaneyulu K (2018). "Non-invasive steel haunch upgradation strategy for seismically deficient reinforced concrete exterior beam-column sub-assemblages". *Steel and Composite Structures*, **28**(6): 719-734. http://dx.doi.org/10.12989/scs.2018.28.6.719

14 Kanchanadevi A and Ramanjaneyulu K (2019). "Non-invasive hybrid retrofit for seismic damage mitigation of gravity load designed exterior beam-column sub-assemblage". *Journal of Earthquake Engineering*. https://doi.org/10.1080/13632469.2019.1592790

15 Zabihi A, Tsang H, Gad EF and Wilson JL (2019). "Design procedure for seismic retrofit of RC beam-column joint using single diagonal haunch". *Structural Engineering and Mechanics*, **71**(4): 341-350. http://dx.doi.org/10.12989/sem.2019.71.4.341

16 Zabihi A, Tsang H, Gad EF and Wilson JL (2018). "Seismic retrofit of exterior RC beam-column joint using diagonal haunch". *Engineering Structures*, **174**: 753-767. https://doi.org/10.1016/j.engstruct.2018.07.100

17 Akbar J, Ahmad N and Alam B (2018). "Seismic performance of RC frames retrofitted with haunch technique". *Structural Engineering and Mechanics*, **67**(1): 1-8. http://dx.doi.org/10.12989/sem.2018.67.1.001

18 Ahmad N, Akbar J, Rizwan M, Alam B, Khan AN and Lateef A (2019). "Haunch retrofitting technique for seismic upgrading deficient RC frames". *Bulletin of Earthquake Engineering*, **17**(7): 3895-3932. https://doi.org/10.1007/s10518-019-00638-9

19 Wang B, Zhu S, Xu YL and Jiang H (2018). "Seismic retrofitting of non-seismically designed RC beam-column joints using buckling-restrained haunches: design and analysis". *Journal of Earthquake Engineering*, **22**(7): 1188-1208. https://doi.org/10.1080/13632469.2016.1277441

20 Ilyas B, Ahmad N, Gul MAA and Ullah A (2019). "Retrofitting of damaged gravity designed reinforced concrete exterior connection using energy dissipating haunch". *Proceedings of the 1st Conference on Sustainability in Civil Engineering*, CUST Islamabad, Pakistan.

21 BCP-SP (2007). *"Building Code of Pakistan – Seismic Provisions"*. Ministry of Housing and Works, Islamabad, 268pp. https://www.pec.org.pk/building_code_pakistan.aspx

22 Rizwan M, Ahmad N and Khan AN (2018). "Seismic performance of compliant and non-compliant special moment-resisting reinforced concrete frames", *ACI Structural Journal*, **115**(4): 1063-1073. https://www.concrete.org/publications/internationalconcreteabstractsportal/m/details/id/51702063

23 Ahmad N, Shahzad A, Rizwan M, Khan AN, Ali SM, Ashraf M, Naseer A, Ali Q and Alam B (2019). "Seismic performance assessment of non-compliant SMRF reinforced concrete frame: shake-table test study". *Journal of Earthquake Engineering*, **23**(3): 444-462. https://doi.org/10.1080/13632469.2017.1326426

24 Masoudi M and Khajevand S (2020). "Revisiting flexural overstrength in RC beam-and-slab floor systems for seismic design and evaluation". *Bulletin of Earthquake Engineering*, **18**(11): 5309-5341. https://doi.org/10.1007/s10518-020-00907-y

25 Marchisella A, Muciaccia G, Sharma A and Eligehausen, R (2021). "Experimental investigation of 3d RC exterior joint retrofitted with fully-fastened-haunch-retrofit-solution". *Engineering Structures*, **239**. https://doi.org/10.1016/j.engstruct.2021.112206

26 Jacobsen LS (1960). "Damping in composite structures". *Proceedings of the 2nd World Conference on Earthquake Engineering*, Tokyo and Kyoto, Japan, pp. 1029-1044. https://engineering.purdue.edu/~ce573/Documents/Damping%20in%20composite%20structures_Jacobsen.pdf

27 Priestley MJN, Calvi GM and Kowalsky MJ (2007). *"Displacement Based Seismic Design of Structures"*. IUSS Press, Pavia, Italy 721 pp.

28 FEMA 356 (2000). "*NEHRP Guidelines for the Seismic Rehabilitation of Buildings*". Federal Emergency Management Agency (FEMA), Washington DC, USA, 518pp. https://www.nehrp.gov/pdf/fema356.pdf

29 Ahmad N (2021) "Force-based seismic design of steel haunch retrofit for RC frames". *Earthquakes and Structures*, **20**(20): 133-148. http://dx.doi.org/10.12989/eas.2021.20.2.133

30 Ahmad N, Masoudi M and Salawdeh S (2021). "Cyclic response and modelling of special moment resisting beams exhibiting fixed-end rotation". *Bulletin of Earthquake Engineering,* **19**(1): 203-240. https://doi.org/10.1007/s10518-020-00987-w

31 Rashid M and Ahmad N (2017). "Economic losses due to earthquake-induced structural damages in RC SMRF Structures". *Cogent Engineering*, **4**(1): 1-15. https://doi.org/10.1080/23311916.2017.1296529

32 Bokor B, Sharma A and Hofmann J (2019). "Experimental investigations on concrete cone failure of rectangular and non-rectangular anchor groups". *Engineering Structures*, **188**: 202-217. https://doi.org/10.1016/j.engstruct.2019.03.019

33 Ahmad N, Shahzad A, Ali Q, Rizwan M and Khan AN (2018). "Seismic fragility functions for code compliant and non-compliant RC SMRF structures in Pakistan". *Bulletin of Earthquake Engineering*, **16**(10): 4675-4703. https://doi.org/10.1007/s10518-018-0377-x

34 ASCE-7-16 (2017). "*Minimum Design Loads and Associated Criteria for Buildings and Other Structures"*. American Society of Civil Engineers, Reston, Virginia, 889pp. http://ASCE7.online

35 Ahmad N and Masoudi M (2020). "Eccentric steel brace retrofit for seismic upgrading of deficient reinforced concrete frames". *Bulletin of Earthquake Engineering*, **18**(6): 2807-2841. https://doi.org/10.1007/s10518-020-00808-0